

# Production of $Z$ boson pairs via gluon fusion in the minimal supersymmetric model

M. S. Berger

*Department of Physics, Indiana University, Bloomington, Indiana 47405*

Chung Kao

*Department of Physics, University of Wisconsin, Madison, Wisconsin 53706*

(Received 2 September 1998; published 2 March 1999)

We present the full one-loop calculation for  $gg \rightarrow ZZ$  in the minimal supersymmetric standard model (MSSM) including nonresonant contributions from the squark loop diagrams and provide analytical expressions for the helicity amplitudes. The one-loop process  $gg \rightarrow ZZ$  via quark loops has been calculated in the standard model. In supersymmetric models, additional contributions arise from squark loops. In some regions of the MSSM parameter space, the top and bottom squark loops can make important contributions to the diagrams involving Higgs bosons. The heavy Higgs scalar ( $H$ ) might be detected at the CERN Large Hadron Collider via  $gg \rightarrow H \rightarrow ZZ$  for  $\tan \beta \lesssim 5$ . [S0556-2821(99)00707-9]

PACS number(s): 12.60.Jv, 13.85.Qk, 14.70.Hp, 14.80.Bn

## I. INTRODUCTION

One of the main purposes for constructing a hadron supercollider is to discover the mechanism responsible for the spontaneous breaking of the electroweak symmetry. A large amount of attention has been devoted recently to the ability of detecting a Higgs boson at the CERN Large Hadron Collider (LHC). Gluon fusion is the main mechanism of producing Higgs bosons at the LHC, and if a  $CP$ -even Higgs scalar is sufficiently heavy it can decay into  $Z$  boson pairs. In the standard model, this is a useful detection channel for the Higgs boson with a mass  $M_{H_{SM}} \gtrsim 2M_Z$  since the  $H_{SM}ZZ$  coupling grows with Higgs boson mass.

The physical Higgs bosons of the minimal supersymmetric extension to the standard model (MSSM) are comprised of two  $CP$ -even states, a lighter  $h$  and a heavier  $H$ , one  $CP$ -odd state,  $A$ , and two charged Higgs bosons  $H^\pm$ . The Higgs potential is constrained by supersymmetry such that all tree-level Higgs boson masses and couplings are determined by just two independent parameters, commonly chosen to be the mass of the  $CP$ -odd pseudoscalar ( $m_A$ ) and the ratio of vacuum expectation values (VEVs) of Higgs fields ( $\tan \beta \equiv v_2/v_1$ ). The  $CP$ -even states can couple to the  $ZZ$  final state at the tree level, but only the heavier one ( $H$ ) can be massive enough to decay into on-shell  $Z$  bosons. For  $m_H \sim m_A \gtrsim 2m_t$ , discovery of the MSSM heavy Higgs scalar in the  $ZZ$  channel could be problematic due to the fact that the Higgs couplings to the gauge bosons arise from the D-term contributions to the scalar potential. As the  $H$  becomes heavy, its coupling with the gauge bosons becomes smaller. Previous studies have found that the production rate for  $gg \rightarrow H \rightarrow ZZ$  is large enough to make this channel a viable one for Higgs detection provided  $\tan \beta \equiv v_2/v_1$  is relatively small ( $\lesssim 5$ ) and that the Higgs boson is not too heavy ( $m_H \lesssim 350$  GeV) [1–4]. The impact of supersymmetric decay modes has also been investigated [2].

The production cross section of  $gg \rightarrow \phi$  ( $\phi = H, h, A$ , and  $H_{SM}$ ) has been studied in increasing detail in the last few years, with much attention devoted to the standard model

Higgs boson or to the lighter MSSM Higgs scalar,  $h$ . The impact of squark loops in the production process has been included, and the impact of squark mixing has been investigated [5]. The QCD corrections to the production process have been calculated and shown to give a large enhancement to the cross section [6].

It is well known [7,8] that the dominant background to the channel  $gg \rightarrow H_{SM} \rightarrow ZZ$  in the standard model are  $q\bar{q} \rightarrow ZZ$ , and the one-loop continuum production of  $Z$  pairs via quark loops,  $gg \rightarrow ZZ$ . In the MSSM the existence of the scalar partners to the quarks gives a new contribution to the continuum production that can interfere with the quark loops and possibly affect the overall level of background. If the masses of the squarks are much larger than the electroweak scale, their contributions to the signal should be small as their mass arises from soft terms rather than from the Higgs mechanism. For squarks with masses comparable to the electroweak scale, significant contributions to the Higgs production signal might be expected. It has been shown [5,9,10] that the squark loops can have a significant impact on the production cross section if the squarks are fairly light. Therefore, a natural step is to also investigate the impact of the squark loops on the background.

The Feynman diagrams for the background coming from squark loops to the Higgs signal in the channel  $gg \rightarrow H \rightarrow ZZ$  are shown in Fig. 1. Since only the third generation gives a sizable contribution to the resonant Higgs contribution  $gg \rightarrow H \rightarrow ZZ$ , one might expect an important contribution from the continuum background for which all three generation squarks are expected to contribute. The central issue concerning the detectability of the Higgs boson is whether the squark loop contribution can be comparable to the quark loop contribution for energies near the Higgs mass. The squark loop contribution is maximal near the production threshold ( $\sqrt{s} = 2m_{\tilde{q}}$ ), so we are most interested in the size of the squark loop background for  $2m_{\tilde{q}} \approx M_H$ .

Another potential application of the process under consideration is a measurement of the  $Hgg$  coupling. The production mechanism involves a coupling to the Higgs boson (a

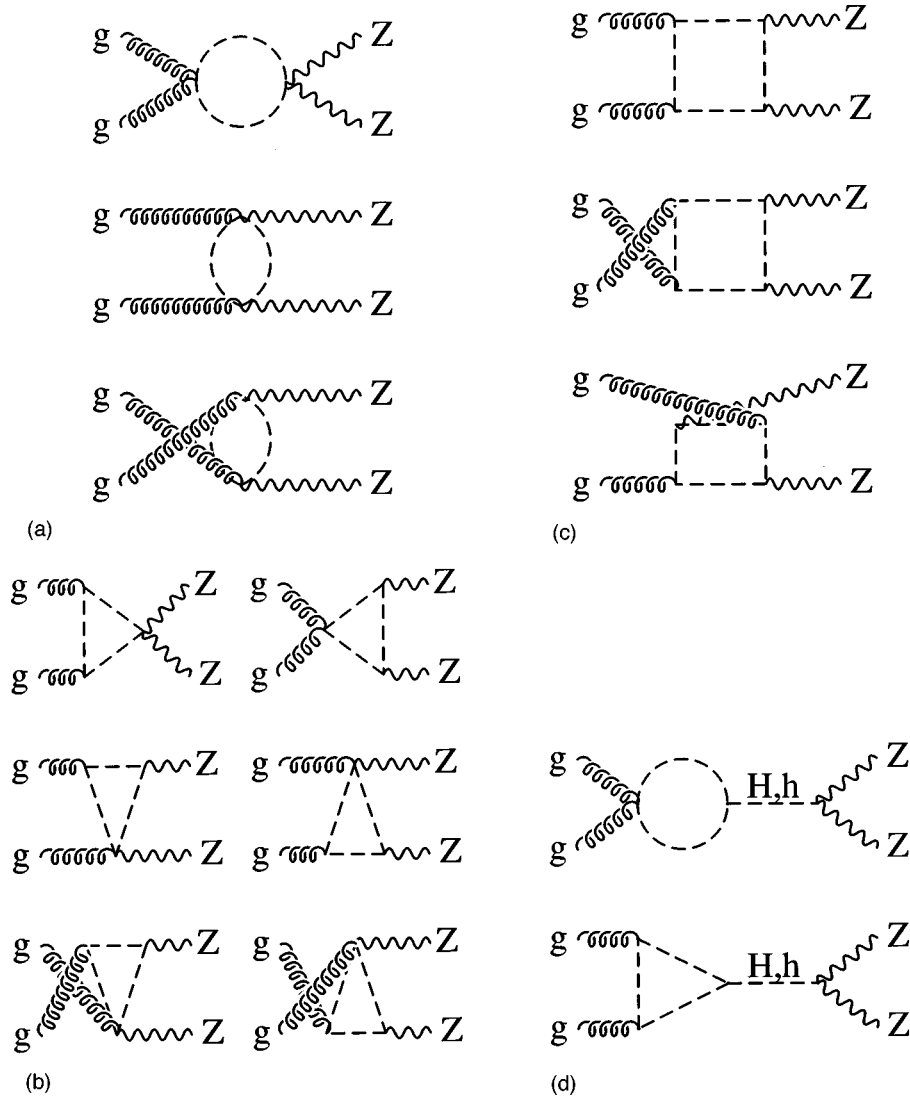


FIG. 1. Feynman diagrams of  $gg \rightarrow ZZ$ : (a) the bubble diagrams, (b) the triangle diagrams, (c) the box diagrams, and (d) the diagrams involving the Higgs bosons.

Yukawa coupling) that implies that only the third generation matter make a sizeable contribution to the rate. Each generation contributes equally to the background (assuming equal masses for squarks in different generations), so potentially there is an enhancement as there is in the case of quark loops. A large background from squark loops could conceivably alter the regions of parameter space (the  $M_A - \tan \beta$  plane) for which the heavy Higgs boson can be discovered.

The gluon coupling to the Higgs boson is mediated by triangle graphs. The calculation of the background involves box graphs and is significantly more complicated than that of the Higgs production cross section. The one-loop integrals, which are expressible in terms of Spence functions (dilogarithms) [11,12], were evaluated numerically using a FORTRAN code [13]. We have not included squark mixing in this first survey, and leave the more general case to a future paper [14]. However we do not expect squark mixing to have a significant effect on the cross sections. While the cross section for the resonant Higgs graphs can be significantly increased by an enhanced  $H\tilde{t}_1\tilde{t}_1$  coupling [10], squark mix-

ing results only in mixing angle factors in the couplings of squarks to the Z bosons and splits the degeneracy of the squark masses for the nonresonant graphs. One expects an enhanced contribution only from the loops involving  $\tilde{t}_1$  squarks which might have a suppressed mass with significant mixing. If the lightest squark is less than half the mass of the Higgs boson, then the Higgs boson can decay into squark pairs making the Higgs boson width broader and more difficult to detect in the  $ZZ$  final state.

## II. THE SQUARK LOOP CONTRIBUTION TO THE BACKGROUND

In this section we compare the size of the squark loop background with that arising from the quark loops. In the standard model, only quark loops contribute to the production of  $ZZ$  from gluon fusion  $gg \rightarrow ZZ$ . In the MSSM there are additional contributions from squark loops, which typically are thought to be suppressed by large squark mass. In this section we present the cross sections expected at the

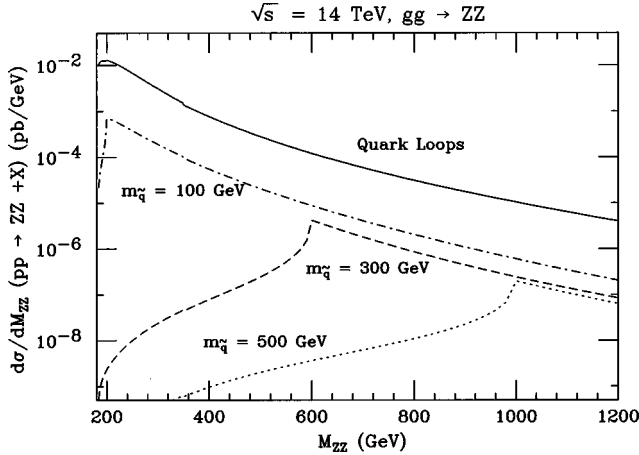


FIG. 2.  $d\sigma/dM_{ZZ}(pp \rightarrow ZZ + X)$ , from  $gg \rightarrow ZZ$ , via squark loops with 12 squarks, without Higgs bosons, for  $m_{\tilde{q}} = 100$  GeV, 300 GeV and 500 GeV. Also shown are the contributions from the box diagrams of quark loops. These contributions are independent of  $\tan \beta$  for fixed squark mass  $m_{\tilde{q}}$ .

LHC with  $\sqrt{s_{pp}} = 14$  TeV. In our numerical computations we use the CTEQ3L parton distribution functions [15] with  $\Lambda_4 = 0.177$  GeV. We take  $\alpha^{-1} = 128$ ,  $\sin^2 \theta_W = 0.2319$ ,  $\alpha_s(M_Z) = 0.119$  and  $m_t = 175$  GeV.

In Fig. 2 we plot the invariant mass distribution  $d\sigma/dM_{ZZ}(pp \rightarrow ZZ + X)$  from  $gg \rightarrow ZZ$  via the squark loops in the MSSM, assuming their masses are all degenerate at values of 100 GeV, 300 GeV and 500 GeV. The lightest squark considered is excluded by the Tevatron data [16], but we include it for comparison purposes. There is a rapid rise in the cross section until the threshold of real squark pair production after which the cross section falls again. Since the squark loop cross section peaks at  $\sqrt{s} \sim 2m_{\tilde{q}}$ , the largest contribution to the background from the squarks comes at subprocess ( $gg \rightarrow ZZ$ ) energies slightly below the squark production threshold. The contribution to  $gg \rightarrow ZZ$  from graphs with squark loops not involving the Higgs boson is separately gauge invariant, and the cross section falls off rapidly as  $\sqrt{s}$  increases.

In Fig. 3 we show the squark loop cross section for the polarization states  $LL$ ,  $TT$  and  $TL+LT$  of the  $ZZ$  final state. The contribution from squark loops is always smaller than that from quark loops even for squarks as light as 100 GeV. The transversely polarized case dominates over the other modes for the squark loops just as it does for the contributions from the quark loops.

### III. THE SUPERSYMMETRIC LIMIT

Some contributions to the one-loop amplitudes for squark loops given in the Appendix are closely related to parts of the helicity amplitudes for the quark loops. These types of supersymmetric relationships [17] were observed in the explicitly computed weak interaction process  $Z \rightarrow 3\gamma$  or equivalently  $\gamma\gamma \rightarrow \gamma Z$  [18], and for  $\gamma\gamma \rightarrow \gamma\gamma$  [19]. One can also compare the contributions from fermion loops in the process  $\gamma\gamma \rightarrow HH$  [20] to the contribution that was obtained

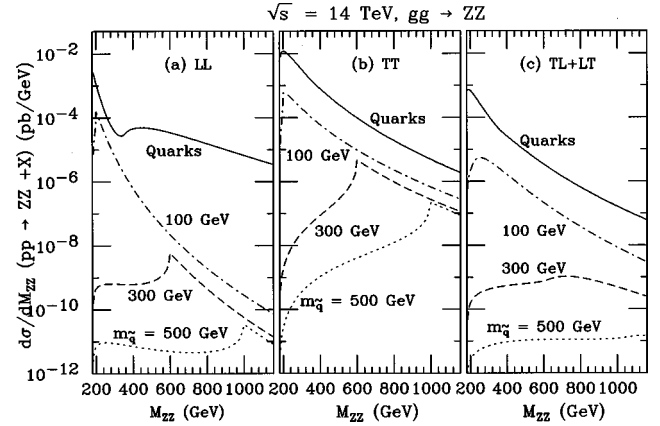


FIG. 3.  $d\sigma/dM_{ZZ}(pp \rightarrow ZZ + X)$ , from  $gg \rightarrow ZZ$ , via squark loops with 12 squarks, without Higgs bosons, in the (a)  $LL$ , (b)  $TT$  and (c)  $TL+LT$  states of the  $ZZ$  for  $m_{\tilde{q}} = 100$  GeV, 300 GeV and 500 GeV.

later for the gauge boson loops [21]. However the most numerically significant contributions to the cross section is often those contributions that are not given by the supersymmetric relationship. In fact the asymptotic behavior ( $\sqrt{s} \rightarrow \infty$ ) is governed by the spin of the particles exchanged in the  $t$ - and  $u$ -channels. For example, one has the dominance of the  $W$  boson loops over fermion loops in the process  $\gamma\gamma \rightarrow ZZ$  [22].

For the process  $gg \rightarrow ZZ$  discussed in this paper, the SUSY relationship exists between the squark loop amplitudes and the parts of the quark loop amplitudes arising from the vector coupling of the  $Z$  boson to quarks. This relationship provides another consistency check on our analytic results in addition to the usual check of gauge invariance. In Fig. 4 the contributions from the top quark loops is compared to the contributions from  $\tilde{t}_L$  and  $\tilde{t}_R$  loops for masses set equal to  $m_t = m_{\tilde{t}} = 175$  GeV.

### IV. INTERFERENCE EFFECTS

In Fig. 5 we present the contributions to  $gg \rightarrow ZZ$  including both the resonant Higgs graphs and the nonresonant

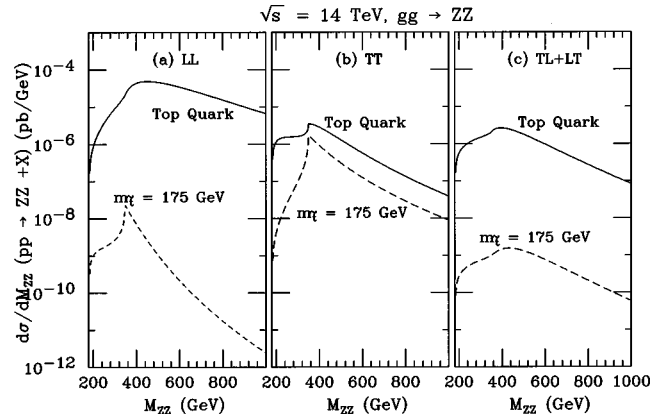


FIG. 4. Differential cross section of  $pp \rightarrow ZZ + X$  from  $gg \rightarrow ZZ$  via top quark and top squark loops without Higgs bosons for  $m_t = m_{\tilde{t}} = 175$  GeV.

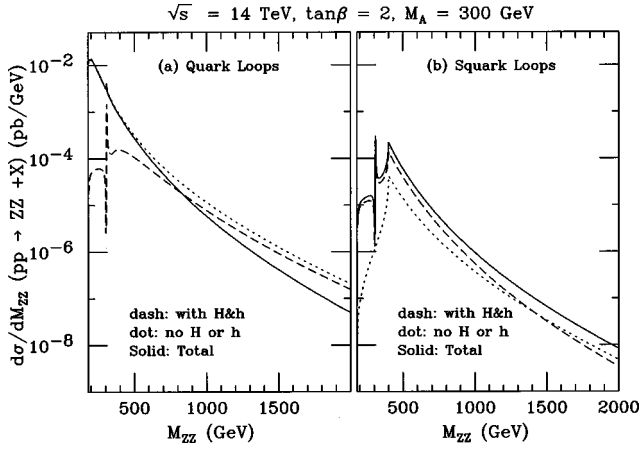


FIG. 5. Differential cross section of  $pp \rightarrow ZZ+X$  from  $gg \rightarrow ZZ$  via (a) quark loops alone and (b) squark loops alone. The dashed lines are the contributions from the Higgs graphs, the dotted lines are the contribution from the nonresonant graphs, and the solid lines are the total.

graphs for the quark loops alone and for the squark loops alone with  $\tan\beta=2$  and 10. The squark mass is 200 GeV, and  $M_A$  is 300 GeV for which  $M_H \approx 309$  GeV. For  $\tan\beta > 5$  the differential cross section appears the same apart from the size of the Higgs boson resonance.

An interesting property of the quark loop amplitudes is the cancellation of the Higgs graphs with the box diagrams which can be related to the good high energy behavior of  $t\bar{t} \rightarrow ZZ$ . The relative sign between the triangle and the box diagrams has been checked with the unitarity condition. We can cut the loop diagrams and obtain the tree processes  $t\bar{t} \rightarrow ZZ$  and  $b\bar{b} \rightarrow ZZ$ . Unitarity then requires a cancellation among tree diagrams at high energy. No such cancellation is required for the scalar loops between diagrams with and without Higgs bosons.

In Fig. 6 we have plotted the contributions to  $gg \rightarrow ZZ$  including both the resonant Higgs graphs and the nonresonant graphs for  $\tan\beta=2$  and 10 including both the quark loops and the squark loops. The background from squark loops can be safely neglected around the Higgs pole region.

The  $H$  resonance exhibits destructive interference just below the peak. This arises from interference with the contribution from the diagrams involving the light Higgs boson  $h$ . This feature is present for squark loops alone and also for quark loops alone, and should be present in nonsupersymmetric extensions of the standard model with extended Higgs sectors. In the MSSM it seems unlikely that this interference dip can be seen experimentally given the size of the underlying background. We note that the contributions to  $gg \rightarrow ZZ$  from squarks loops without Higgs bosons are also valid in nonminimal supersymmetric models since they do not involve contributions from the Higgs sector.

## V. HIGGS SEARCH AT THE CERN LHC

The basic features that arise from the numerical calculations are that the squark production cross section peak near

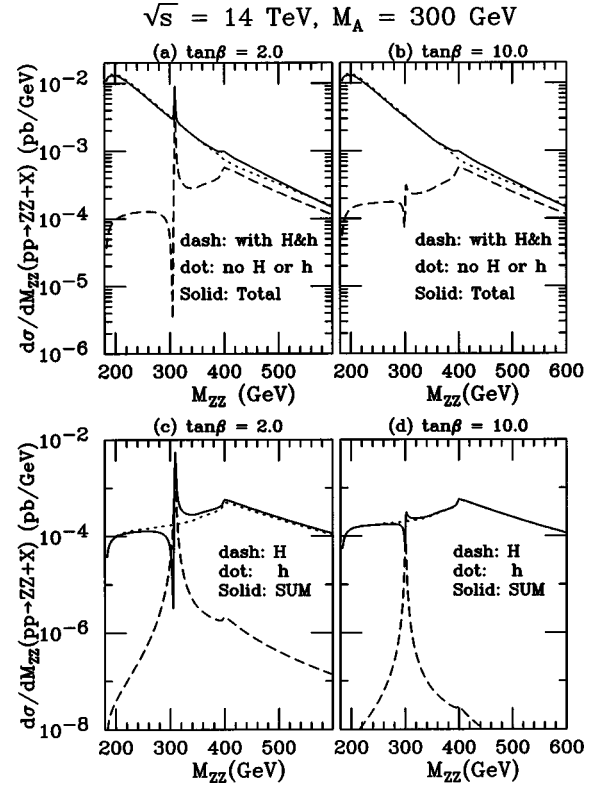


FIG. 6. Differential cross section of  $pp \rightarrow ZZ+X$  from  $gg \rightarrow ZZ$  via both quark and squark loops, for  $m_{\tilde{q}} = 200$  GeV, as a function of  $M_{ZZ}$ , for (a)  $\tan\beta=2$  and (b)  $\tan\beta=10$ . Also presented is the destructive interference between diagrams with the  $H$  and the  $h$  for (c)  $\tan\beta=2$  and (d)  $\tan\beta=10$ .

the real production thresholds,  $\sqrt{s} \sim 2m_{\tilde{q}}$ . This enhancement should be smoothed somewhat after the inclusion of QCD corrections. The overall level of the squark loop contribution is much smaller than that of the quark loops, and even after including the interference between the two contributions we find that the squark loops can always be safely neglected in an overall estimate of the background level.

In Fig. 7, we present the invariant mass distribution of  $ZZ$  including the Higgs signal from gluon fusion and the irreducible background from  $q\bar{q}$  annihilation and  $gg$  fusion via quark and squark loops in  $pp$  collisions, with a rapidity cut  $|y_Z| < 2.5$ , for  $m_{\tilde{q}} = 200$  GeV,  $\tan\beta=2$  and  $\tan\beta=10$ . For the smaller values of  $\tan\beta$  near 2, pronounced peaks appear at  $M_{ZZ} = M_H$ . For  $\tan\beta \geq 10$ , the Higgs peaks become almost invisible.

The Higgs signal in the ‘‘gold-plated’’ mode  $H \rightarrow ZZ \rightarrow 4l$  is viable for  $\tan\beta \leq 5$  when there are no supersymmetric decays of the Higgs boson [2]. The ‘‘silver-plated’’ mode  $H \rightarrow ZZ \rightarrow l^+ l^- \nu \bar{\nu}$  might also be used, and has a rate six times that of the gold-plated mode, but reducible  $Z$ -jet backgrounds might be a problem [23,3]. If real squarks can be produced the Higgs width becomes larger, the Higgs peak in the invariant mass of  $ZZ$  is reduced and the event rate is too small to discover the Higgs boson. Even if we choose squarks with a mass such that the squark contribution peaks near the Higgs pole, the contribution to the continuum background from the squark loops is negligible.

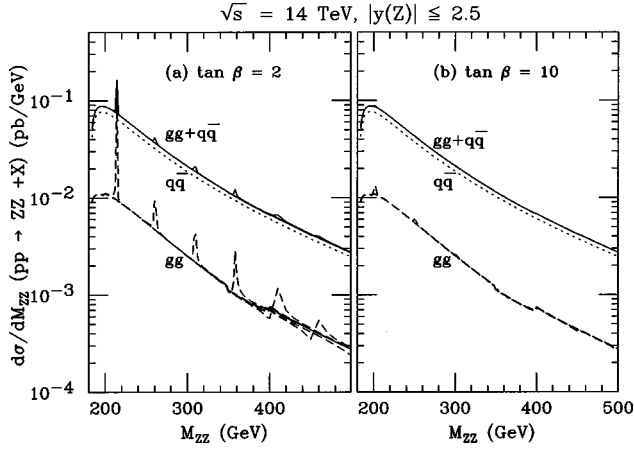


FIG. 7. Differential cross section of the Higgs signal in  $pp$  collisions with a rapidity cut  $|y_Z| < 2.5$ , from quark and squark loops, for  $m_{\tilde{q}} = 200$  GeV, as a function of  $M_{ZZ}$ , for  $\tan\beta=2$  and 10; and, the irreducible background  $d\sigma/dM_{ZZ}$  via  $q\bar{q}$  annihilation and  $gg$  fusion.

We expect that the squark loop background is also negligible for Higgs bosons with masses  $M_{H,h} < 2M_Z$ , so that at least one of the  $Z$  bosons is virtual ( $Z^*$ ). In fact for the lighter supersymmetric Higgs,  $h$ , this is an attractive channel for discovery at the LHC [4]. The calculation  $gg \rightarrow ZZ^* \rightarrow 4l$  has been performed for the quark loops in Ref. [24], and that background falls rapidly for invariant masses decreasing below the  $ZZ$  threshold. We expect the squark loops to be negligible in this case as well, but our calculation is applicable only for real  $Z$  bosons.

## VI. CONCLUSIONS

We have calculated the contribution from squark loops to the process  $gg \rightarrow ZZ$  at the LHC. We find that they are substantially smaller than the contribution from quark loops, and can usually be safely neglected in computation of the continuum background in the Higgs search. In models with two  $CP$ -even Higgs bosons, we have also shown the amplitudes involving the heavy Higgs boson interferes destructively just below the resonance with the contributions from the light Higgs bosons. The expressions for the helicity amplitudes given in the appendix can be easily adapted to give the squark loop contributions to the processes  $gg \rightarrow \gamma\gamma$ ,  $\gamma\gamma \rightarrow \gamma\gamma$  and  $\gamma\gamma \rightarrow ZZ$ . The first process is relevant for Higgs searches at the LHC, while the last two are relevant for the  $\gamma\gamma$  options of future linear  $e^+e^-$  colliders.

## ACKNOWLEDGMENTS

This research was supported in part by the U.S. Department of Energy under Grants No. DE-FG02-95ER40661 and No. DE-FG02-95ER40896 and in part by the University of Wisconsin Research Committee with funds granted by the Wisconsin Alumni Research Foundation.

## APPENDIX

In this appendix we give the formulas for the helicity amplitudes. We define helicity vectors for the process (12  $\rightarrow$  34) as

$$e_1^+ = e_2^- = \frac{1}{\sqrt{2}}(0; -i, 1, 0), \quad (\text{A1})$$

$$e_1^- = e_2^+ = \frac{1}{\sqrt{2}}(0; i, 1, 0), \quad (\text{A2})$$

$$e_3^+ = e_4^- = \frac{1}{\sqrt{2}}(0; i \cos \theta, 1, -i \sin \theta), \quad (\text{A3})$$

$$e_3^- = e_4^+ = \frac{1}{\sqrt{2}}(0; -i \cos \theta, 1, i \sin \theta), \quad (\text{A4})$$

$$e_3^0 = \frac{1}{m_Z}(q; p \sin \theta, 0, p \cos \theta), \quad (\text{A5})$$

$$e_4^0 = \frac{1}{m_Z}(q; -p \sin \theta, 0, -p \cos \theta), \quad (\text{A6})$$

where the momenta are defined as

$$p_1^\mu = (p; 0, 0, p), \quad (\text{A7})$$

$$p_2^\mu = (p; 0, 0, -p), \quad (\text{A8})$$

$$p_3^\mu = (p; q \sin \theta, 0, q \cos \theta), \quad (\text{A9})$$

$$p_4^\mu = (p; -q \sin \theta, 0, -q \cos \theta), \quad (\text{A10})$$

in the  $gg$  rest frame. One then can define the Mandelstam variables

$$s = (p_1 + p_2)^2, \quad t = (p_1 - p_3)^2, \quad u = (p_1 - p_4)^2. \quad (\text{A11})$$

In nonsupersymmetric extensions of the Higgs sector the adjustment to the calculations is clearly only in the diagrams containing the Higgs bosons for which the single  $s$ -channel contribution is replaced by multiple  $s$ -channel Higgs contributions with couplings that preserve the unitarity cancellations that occur in the standard model. Indeed in the MSSM the unitarity cancellation in the quark loop diagrams alone manifests itself as the contribution for the  $h$  and  $H$  Higgs bosons. The standard model contribution from quark loops to the production of longitudinal pairs (apart from an overall factor)

$$\mathcal{A}_{++00}^{\text{Higgs}} = \frac{2m_q^2}{s - m_H^2 + i\Gamma_H m_H} \frac{s_2}{2m_Z^2} (-2 + s_4 C_0(s)), \quad (\text{A12})$$

becomes

$$\mathcal{A}_{++++}^{\text{Higgs}} = \frac{s_2}{2m_Z^2} (-2 + s_4 C_0(s)) \left[ \frac{2m_q^2}{s - m_h^2 + i\Gamma_h m_h} \frac{\cos \alpha \sin(\beta - \alpha)}{\sin \beta} + \frac{2m_q^2}{s - m_H^2 + i\Gamma_H m_H} \frac{\sin \alpha \cos(\beta - \alpha)}{\sin \beta} \right], \quad (\text{A13})$$

for up-type quarks, and

$$\mathcal{A}_{++++}^{\text{Higgs}} = \frac{s_2}{2m_Z^2} (-2 + s_4 C_0(s)) \left[ -\frac{2m_q^2}{s - m_h^2 + i\Gamma_h m_h} \frac{\sin \alpha \sin(\beta - \alpha)}{\cos \beta} + \frac{2m_q^2}{s - m_H^2 + i\Gamma_H m_H} \frac{\cos \alpha \cos(\beta - \alpha)}{\cos \beta} \right], \quad (\text{A14})$$

for down-type quarks in the MSSM.

Extracting an overall factor

$$\frac{2\alpha_s \alpha}{\sin^2 \theta_w \cos^2 \theta_w} (L^2 + R^2) \quad (\text{A15})$$

where

$$L = \frac{1}{2} - \frac{2}{3} \sin^2 \theta_w, \quad (\text{A16})$$

$$R = \frac{2}{3} \sin^2 \theta_w, \quad (\text{A17})$$

for charge 2/3 squarks and where

$$L = -\frac{1}{2} + \frac{1}{3} \sin^2 \theta_w, \quad (\text{A18})$$

$$R = -\frac{1}{3} \sin^2 \theta_w, \quad (\text{A19})$$

for charge  $-1/3$  squarks, the helicity amplitudes for squark loop diagrams for the process  $gg \rightarrow ZZ$  not involving the Higgs bosons are

$$\begin{aligned} \mathcal{A}_{+--+} = & \left\{ D(s, t) \left( \frac{st^2}{Y} + 2m_q^2 \right) \left( m_q^2 + \frac{m_Z^4}{s_4} \right) + C(t) \left[ \frac{2m_q^2 s_2}{s_4} \left( \frac{u_1}{s} - \frac{m_Z^2}{t_1} \right) - 2 \frac{tt_1}{Y} \left( m_q^2 + \frac{m_Z^4}{s_4} \right) \right] + B(t) \frac{m_Z^2}{s_4 t_1^2} (Y + 2m_Z^2 t) + (t \leftrightarrow u) \right\} \\ & + D(t, u) m_q^2 \left( 2m_q^2 + \frac{s_2 Y}{s s_4} \right) + C_0(s) \left( \frac{s s_2}{Y} \right) \left( m_q^2 + \frac{m_Z^4}{s_4} \right) + C(s) \left( \frac{t^2 + u^2 - 2m_Z^4}{Y} \right) \left( m_q^2 + \frac{m_Z^4}{s_4} \right) - \frac{Y}{t_1 u_1} \left( 1 + 2 \frac{m_Z^2}{s_4} \right), \quad (\text{A20}) \end{aligned}$$

$$\begin{aligned} \mathcal{A}_{+--+} = & \left\{ D(s, t) \left[ 2m_q^2 \left( m_q^2 - \frac{m_Z^4}{s_4} \right) + \frac{m_q^2 s t^2}{Y} \right] + C(t) \left[ 2 \frac{m_Z^2 t_1 Y}{s^2 s_4} - 2m_q^2 \left[ 1 + \frac{m_Z^2 s_2}{s_4 t_1} + \frac{t_1}{s} \right] - 2m_q^2 \frac{t t_1}{Y} \right] - B(t) m_Z^2 \left( 2 \frac{t}{s} - 1 \right) \frac{Y}{s_4 t_1^2} \right. \\ & \left. + (t \leftrightarrow u) \right\} + D(t, u) \left( \frac{Y}{s} + 2m_q^2 \right) \left( m_q^2 - \frac{Y m_Z^2}{s s_4} \right) + C_0(s) \left( \frac{s_2 m_q^2}{s_4 Y} \right) (t^2 + u^2 - 2m_Z^4) + C(s) \frac{s s_4 m_q^2}{Y} - \frac{Y}{t_1 u_1} \left( 1 + 2 \frac{m_Z^2}{s_4} \right), \quad (\text{A21}) \end{aligned}$$

$$\begin{aligned} \mathcal{A}_{+-00} = & \left\{ D(s, t) \frac{s m_Z^2}{s_4} \left( m_q^2 + \frac{st^2}{2Y} \right) + C(t) \frac{m_Z^2}{s_4} \left[ 8 \frac{m_q^2 Y}{s t_1} - \frac{s t t_1}{Y} \right] - B(t) 2 \frac{m_Z^2}{s_4 t_1^2} (t^2 + m_Z^4) + (t \leftrightarrow u) \right\} - D(t, u) \frac{(t-u)^2 m_Z^2 m_q^2}{s s_4} \\ & + C_0(s) \left( \frac{s^2 s_2 m_Z^2}{2 s_4 Y} \right) + C(s) \left( \frac{s m_Z^2}{2 s_4 Y} \right) (t^2 + u^2 - 2m_Z^4) - \frac{4 m_Z^2 Y}{s_4 t_1 u_1}, \quad (\text{A22}) \end{aligned}$$

$$\begin{aligned}
 \mathcal{A}_{++00} = & \left\{ D(s,t) \frac{sm_Z^2 m_q^2}{s_4} + C(t) m_Z^2 \left( \frac{(t-u)^2 t_1}{s^2 s_4} + 8 \frac{m_Z^2 m_q^2}{s_4 t_1} \right) - B(t) \frac{m_Z^2}{s_4} \left( 4 \frac{t}{s} + 2 - 4 \frac{m_Z^4}{t_1^2} \right) + (t \leftrightarrow u) \right\} \\
 & - D(t,u) \frac{m_Z^2 (t-u)^2}{2s^2 s_4} (Y + 2m_Z^2 s) + C_0(s) \left( 8 \frac{m_Z^2 m_q^2}{s_4} \right) + \frac{4m_Z^2 Y}{s_4 t_1 u_1}, \tag{A23}
 \end{aligned}$$

$$\begin{aligned}
 \mathcal{A}_{+--+} = & \left\{ D(s,t) \left[ \frac{1}{2s_4 Y^2} (2m_q^2 Y + st^2)(2m_q^2 s_4 Y + ss_4 t^2 - 2m_Z^4 Y) + \beta_s \frac{st}{2s_4 Y^2} (4m_q^2 Y + st^2)(t^2 - m_Z^4 + Y) \right] + C(t) \right. \\
 & \times \left[ 2m_q^2 \frac{1}{ss_4 t_1 Y} (m_Z^2 Y(t^2 + u^2 - 2m_Z^4) - ss_4 t t_1^2) + \frac{t t_1}{s_4 Y^2} (2m_Z^4 Y - ss_4 t^2) + \beta_s \left\{ 2m_q^2 \frac{s}{s_4 t_1 Y} (t(t^2 - m_Z^4) - m_Z^2 Y) \right. \right. \\
 & \left. \left. - \frac{st^2 t_1}{s_4 Y^2} (t^2 - m_Z^4 + Y) \right\} \right] + B(t) \left[ 2 \frac{m_Z^4}{s_4 t_1} + \frac{m_Z^4}{t_1^2} \left( 1 + 2 \frac{m_Z^2}{s_4} \right) - \frac{1}{2} + \frac{m_Z^2}{s_4} - \beta_s \left( 2 \frac{m_Z^4}{s_4 t_1} + m_Z^4 \frac{s}{s_4 t_1^2} + 2 \frac{t}{s_4} - \frac{1}{2} \right) \right. \\
 & \left. - \frac{t^2}{Y} \left( 1 + \frac{\beta_s (t-u)}{s_4} \right) \right] + (t \leftrightarrow u, \beta_s \rightarrow -\beta_s) \left\{ D(t,u) 2m_q^2 \left( m_q^2 - \frac{m_Z^2 Y}{ss_4} \right) \right. \\
 & \left. + C_0(s) \frac{ss_2}{Y} \left[ m_q^2 + \frac{[(t^2 + u^2 - 2m_Z^4)(t^2 + tu + u^2 - 2m_Z^4) - 2Y^2]}{2s_4 Y} + \beta_s \frac{t-u}{s_4} \left\{ m_q^2 + \frac{s(t^2 + tu + u^2 - 2m_Z^4)}{2Y} \right\} \right] \right. \\
 & \left. + C(s) \frac{s}{Y} \left[ m_q^2 s_4 + \frac{t^2(t^2 - m_Z^4 + Y) + u^2(u^2 - m_Z^4 + Y)}{2Y} + \beta_s (t-u) \right. \right. \\
 & \left. \left. \times \left\{ m_q^2 + \frac{t^2(t^2 - m_Z^4 + Y) + u^2(u^2 - m_Z^4 + Y) + 2(s_2^2 - m_Z^4)Y}{2s_4 Y} \right\} \right] \right. \\
 & \left. + B(s) \left[ \left( \frac{s_2(t^2 + u^2 - 2m_Z^4 + Y)}{s_4 Y} \right) + \beta_s \left( \frac{ss_2(t-u)}{s_4 Y} \right) \right] + \frac{1}{s_4 t_1 u_1} [s_2 Y + \beta_s m_Z^2 s(t-u)], \right. \tag{A24}
 \end{aligned}$$

$$\begin{aligned}
 \mathcal{A}_{+++0}/\Delta = & \left\{ D(s,t) \frac{sm_q^2}{2s_4} (t^2 - m_Z^4 + Y) + C(t) \left[ m_q^2 \frac{s(t^2 - m_Z^4 + Y)}{s_4 t_1} + \frac{(t-u)t_1 Y}{2ss_4} + \beta_s \left\{ m_q^2 \frac{s(t^2 - m_Z^4 + Y) + t_1^2(t-u)}{s_4 t_1} \right. \right. \right. \\
 & \left. \left. + \frac{t_1(t-u)Y}{2ss_4} \right\} \right] + B(t) (1 + \beta_s) \frac{sY}{2s_4} \left[ \frac{m_Z^2}{t_1} \left( \frac{1}{t_1} - \frac{2}{s} \right) - \frac{2}{s} \right] - (t \leftrightarrow u) \left\{ -D(t,u) \frac{Y(t-u)}{4ss_4} [(Y + 2sm_q^2) \right. \\
 & \left. + \beta_s (Y + 4sm_q^2)] - C_0(s) \frac{sm_q^2(t-u)}{s_4} - (1 + \beta_s) \frac{s(t-u)Y}{2s_4 t_1 u_1}, \right. \tag{A25}
 \end{aligned}$$

$$\begin{aligned}
 \mathcal{A}_{+-+0}/\Delta = & \left\{ D(s,t) \left[ \frac{s}{4s_4 Y} (t^2 - m_Z^4 + Y)(2m_q^2 Y + st^2) + \beta_s \frac{s^2 t}{4Y s_4} (4m_q^2 Y + st^2) \right] - C(t) \left[ m_q^2 \frac{(t-u)Y}{s_4 t_1} + \frac{st t_1 (t^2 - m_Z^4 + Y)}{2s_4 Y} \right. \right. \\
 & \left. \left. - \beta_s \left\{ m_q^2 \frac{s(st + 2Y)}{s_4 t_1} - \frac{s^2 t^2 t_1}{2s_4 Y} \right\} \right] + B(t) \frac{s}{2s_4} \left[ m_Z^2 (t-u) \frac{t}{t_1^2} + t + m_Z^2 - \beta_s \left( m_Z^4 \frac{s}{t_1^2} + m_Z^2 \frac{s}{t_1} + t + m_Z^2 \right) \right] \right. \\
 & \left. - (t \leftrightarrow u, \beta_s \rightarrow -\beta_s) \left\{ -D(t,u) \frac{m_q^2 Y(t-u)}{2s_4} - C_0(s) \frac{s^2}{4s_4} \left[ \frac{(t-u)(t^2 + u^2 + 2Y)}{Y} + \beta_s \left( 4m_q^2 + \frac{s(t^2 + u^2)}{Y} \right) \right] \right. \right. \\
 & \left. \left. - C(s) \frac{s^2 s_2}{4Y} \left[ (t-u) + \beta_s \frac{t^2 + u^2 - 2m_Z^4}{s_4} \right] - B(s) \frac{s(t-u + \beta_s s)}{2s_4} + \frac{sY(t-u - s\beta_s)}{2s_4 t_1 u_1}, \right. \right. \tag{A26}
 \end{aligned}$$

$$\begin{aligned}
\mathcal{A}_{++++} = & \left\{ D(s,t) 2m_q^2 \left( m_q^2 + \frac{m_Z^4}{s_4} \right) + C(t) \left[ -2 \frac{m_q^2}{s s_4 t_1} [s_2(t_1(t-u) + Y) - 2m_Z^2 t_1^2] - \frac{s_2 t_1 Y}{s^2 s_4} + \beta_s \left\{ -2m_q^2 \frac{t_1(t-u) + Y}{s_4 t_1} - \frac{t_1 Y}{s s_4} \right\} \right] \right. \\
& + B(t) \left( \frac{(1 + \beta_s)s - 2m_Z^2}{2s_4} \right) \left( 2 \frac{m_Z^4}{t_1^2} - 2 \frac{t}{s} - 1 \right) + (t \leftrightarrow u) \left. \right\} + D(t,u) \frac{1}{2s^2 s_4} [(2sm_q^2 + Y)(2s s_4 m_q^2 + s_2 Y) \\
& + \beta_s s Y(Y + 4sm_q^2)] + C_0(s) 4 \frac{m_Z^2 m_q^2}{s_4} + \frac{1}{s_4 t_1 u_1} [m_Z^2(2Y - s s_4) + \beta_s s Y], \tag{A27}
\end{aligned}$$

where  $s_4 = s - 4m_Z^2$ ,  $s_2 = s - 2m_Z^2$ ,  $t_1 = t - m_Z^2$ ,  $u_1 = u - m_Z^2$ ,  $\beta_s = \sqrt{s_4/s}$ ,  $Y = tu - m_Z^4$ , and  $\Delta = \sqrt{-2m_Z^2/sY}$ . The squark mass-squared is denoted by  $m_q^2$ , where this is the eigenvalue(s) of the squark mass-squared matrix. Different masses for the left- and right-handed squarks can be accounted for by separating the overall factors in Eq. (A15), and using two squark masses  $m_{q_L}^2$  and  $m_{q_R}^2$  in the expressions for the helicity amplitudes above. The factors  $B$ ,  $C$  and  $D$  are the usual scalar integrals that result from the reduction [11,12] of the tensor integrals in the original Feynman diagrams. Expressions for these in terms of logarithms and dilogarithms can be found in Ref. [8]. The other helicity amplitudes are related by the same substitutions required for the quark loops [8]

$$\begin{aligned}
\mathcal{A}_{\lambda_1 \lambda_2 \lambda_3 \lambda_4} &= \mathcal{A}_{-\lambda_1 - \lambda_2 - \lambda_3 - \lambda_4}^*, \\
\mathcal{A}_{+ + - -}(\beta_s) &= \mathcal{A}_{++++}(-\beta_s), \\
\mathcal{A}_{+ + + -}(\beta_s) &= \mathcal{A}_{+ + - +}(\beta_s), \\
\mathcal{A}_{+ - - -}(\beta_s) &= \mathcal{A}_{- - - +}(\beta_s), \\
\mathcal{A}_{+ - - +}(\beta_s) &= \mathcal{A}_{+ - + -}(-\beta_s), \\
\mathcal{A}_{+ + + 0}(\beta_s) &= \mathcal{A}_{+ + 0 +}(\beta_s) = \mathcal{A}_{+ + - 0}(-\beta_s) = \mathcal{A}_{+ + 0 -}(-\beta_s), \\
\mathcal{A}_{+ - + 0}(\beta_s) &= -\mathcal{A}_{+ - 0 +}(-\beta_s) = \mathcal{A}_{+ - - 0}(-\beta_s) = -\mathcal{A}_{+ - 0 -}(\beta_s). \tag{A28}
\end{aligned}$$

The helicity amplitudes for top squark loop diagrams containing the Higgs bosons for the process  $gg \rightarrow ZZ$  are:

$$\begin{aligned}
\mathcal{A}_{++00}^{\text{Higgs}} = & \frac{\alpha_s \alpha}{\sin^2 \theta_w \cos^2 \theta_w} \left[ \left( \frac{2m_t^2 \sin \alpha}{m_W \sin \beta} + \frac{m_Z}{2 \cos \theta_w} \cos(\beta + \alpha) \right) \frac{m_Z}{\cos \theta_w} \frac{s_2}{2m_Z^2} (1 + 2m_q^2 C_0(s)) \frac{\cos(\beta - \alpha)}{s - m_H^2 + i\Gamma_H m_H} + \left( \frac{2m_t^2 \cos \alpha}{m_W \sin \beta} \right. \right. \\
& \left. \left. - \frac{m_Z}{2 \cos \theta_w} \sin(\beta + \alpha) \right) \frac{m_Z}{\cos \theta_w} \frac{s_2}{2m_Z^2} (1 + 2m_q^2 C_0(s)) \frac{\sin(\beta - \alpha)}{s - m_h^2 + i\Gamma_h m_h} \right], \tag{A29}
\end{aligned}$$

$$\begin{aligned}
\mathcal{A}_{++++}^{\text{Higgs}} = & \frac{\alpha_s \alpha}{\sin^2 \theta_w \cos^2 \theta_w} \left[ \left( \frac{2m_t^2 \sin \alpha}{m_W \sin \beta} + \frac{m_Z}{2 \cos \theta_w} \cos(\beta + \alpha) \right) \frac{m_Z}{\cos \theta_w} (1 + 2m_q^2 C_0(s)) \frac{\cos(\beta - \alpha)}{s - m_H^2 + i\Gamma_H m_H} + \left( \frac{2m_t^2 \cos \alpha}{m_W \sin \beta} \right. \right. \\
& \left. \left. - \frac{m_Z}{2 \cos \theta_w} \sin(\beta + \alpha) \right) \frac{m_Z}{\cos \theta_w} (1 + 2m_q^2 C_0(s)) \frac{\sin(\beta - \alpha)}{s - m_h^2 + i\Gamma_h m_h} \right], \tag{A30}
\end{aligned}$$

and the contributions from the bottom squark are:

$$\begin{aligned}
\mathcal{A}_{++00}^{\text{Higgs}} = & \frac{\alpha_s \alpha}{\sin^2 \theta_w \cos^2 \theta_w} \left[ \left( \frac{2m_b^2 \cos \alpha}{m_W \cos \beta} - \frac{m_Z}{2 \cos \theta_w} \cos(\beta + \alpha) \right) \frac{m_Z}{\cos \theta_w} \frac{s_2}{2m_Z^2} (1 + 2m_q^2 C_0(s)) \frac{\cos(\beta - \alpha)}{s - m_H^2 + i\Gamma_H m_H} + \left( -\frac{2m_b^2 \sin \alpha}{m_W \cos \beta} \right. \right. \\
& \left. \left. + \frac{m_Z}{2 \cos \theta_w} \sin(\beta + \alpha) \right) \frac{m_Z}{\cos \theta_w} \frac{s_2}{2m_Z^2} (1 + 2m_q^2 C_0(s)) \frac{\sin(\beta - \alpha)}{s - m_h^2 + i\Gamma_h m_h} \right], \tag{A31}
\end{aligned}$$

$$\begin{aligned}
\mathcal{A}_{++++}^{\text{Higgs}} = & \frac{\alpha_s \alpha}{\sin^2 \theta_w \cos^2 \theta_w} \left[ \left( \frac{2m_b^2 \cos \alpha}{m_W \cos \beta} - \frac{m_Z}{2 \cos \theta_w} \cos(\beta + \alpha) \right) \frac{m_Z}{\cos \theta_w} (1 + 2m_q^2 C_0(s)) \frac{\cos(\beta - \alpha)}{s - m_H^2 + i\Gamma_H m_H} + \left( -\frac{2m_b^2 \sin \alpha}{m_W \cos \beta} \right. \right. \\
& \left. \left. + \frac{m_Z}{2 \cos \theta_w} \sin(\beta + \alpha) \right) \frac{m_Z}{\cos \theta_w} (1 + 2m_q^2 C_0(s)) \frac{\sin(\beta - \alpha)}{s - m_h^2 + i\Gamma_h m_h} \right]. \quad (\text{A32})
\end{aligned}$$

We remark here that the equations above involving transverse  $Z$  bosons can be reduced to the helicity amplitudes for  $gg \rightarrow \gamma\gamma$  from squark loops not involving the Higgs graphs (the process  $gg \rightarrow h \rightarrow \gamma\gamma$  has been investigated including squark mixing in Refs. [5, 10]). Also the contribution to photon-photon scattering  $\gamma\gamma \rightarrow \gamma\gamma$  can be obtained from that for  $gg \rightarrow \gamma\gamma$  by changing overall factors.

- 
- [1] V. Barger, M. S. Berger, R. J. N. Phillips, and A. Stange, *Phys. Rev. D* **45**, 4128 (1992); J. F. Gunion, R. Bork, H. E. Haber, and A. Seiden, *ibid.* **46**, 2040 (1992); Z. Kunszt and F. Zwirner, *Nucl. Phys.* **B385**, 3 (1992).
- [2] H. Baer, M. Bisset, D. Dicus, C. Kao, and X. Tata, *Phys. Rev. D* **47**, 1062 (1993); H. Baer, M. Bisset, C. Kao, and X. Tata, *ibid.* **50**, 316 (1994).
- [3] CMS Technical Proposal, CERN/LHCC 94-38 (1994); Atlas Technical Proposal, CERN/LHCC 94-43 (1994); E. Richter-Was *et al.*, *Int. J. Mod. Phys. A* **13**, 1371 (1998).
- [4] A summary of the many discovery possibilities for weakly coupled Higgs bosons can be found in J. F. Gunion, A. Stange, and S. Willenbrock, UCD-95-28, hep-ph/9602238.
- [5] B. Kileng, *Z. Phys. C* **63**, 87 (1994).
- [6] M. Spira, A. Djouadi, D. Graudenz, and P. M. Zerwas, *Nucl. Phys.* **B453**, 17 (1995); S. Dawson, A. Djouadi, and M. Spira, *Phys. Rev. Lett.* **77**, 16 (1996).
- [7] D. A. Dicus, C. Kao, and W. W. Repko, *Phys. Rev. D* **36**, 1570 (1987).
- [8] E. W. N. Glover and J. J. van der Bij, *Phys. Lett. B* **219**, 488 (1989); *Nucl. Phys.* **B321**, 561 (1989).
- [9] H. König, *Z. Phys. C* **69**, 493 (1996).
- [10] A. Djouadi, *Phys. Lett. B* **435**, 101 (1998).
- [11] G. 't Hooft and M. Veltman, *Nucl. Phys.* **B153**, 365 (1979); G. Passarino and M. Veltman, *ibid.* **B160**, 151 (1979).
- [12] G. J. van Oldenborgh and J. A. M. Vermaseren, *Z. Phys. C* **46**, 425 (1990).
- [13] D. A. Dicus and C. Kao, LOOP, a FORTRAN program for evaluating one-loop integrals.
- [14] M. S. Berger and C. Kao (in preparation).
- [15] H.-L. Lai *et al.*, *Phys. Rev. D* **51**, 4763 (1995).
- [16] CDF Collaboration, F. Abe *et al.*, *Phys. Rev. D* **56**, 1357 (1997); D0 Collaboration, A. Abachi *et al.*, *Phys. Rev. Lett.* **75**, 618 (1995).
- [17] Z. Bern and D. A. Kosower, *Nucl. Phys.* **B379**, 451 (1992); **B379**, 562 (1992); C. S. Lam, *ibid.* **B397**, 143 (1993); Z. Bern, L. Dixon, and D. A. Kosower, *Phys. Rev. Lett.* **70**, 2677 (1993).
- [18] Z. Bern and A. G. Morgan, *Phys. Rev. D* **49**, 6155 (1994).
- [19] G. V. Jikia and A. Tkabladze, *Phys. Lett. B* **323**, 453 (1994).
- [20] E. W. N. Glover and J. J. van der Bij, *Nucl. Phys.* **B309**, 282 (1988).
- [21] G. V. Jikia, *Nucl. Phys.* **B412**, 57 (1994).
- [22] G. V. Jikia, *Phys. Lett. B* **298**, 224 (1993); *Nucl. Phys.* **B405**, 24 (1993); M. S. Berger, *Phys. Rev. D* **48**, 5121 (1993); D. A. Dicus and C. Kao, *ibid.* **49**, 1265 (1994).
- [23] M. S. Chanowitz and M. K. Gaillard, *Nucl. Phys.* **B261**, 379 (1985); R. N. Cahn and M. S. Chanowitz, *Phys. Rev. Lett.* **56**, 1327 (1986).
- [24] C. Zecher, T. Matsuura, and J. J. van der Bij, *Z. Phys. C* **64**, 219 (1994).